

Cite this: *RSC Adv.*, 2016, 6, 87593

Enhanced long-term nitrogen removal by organotrophic anammox bacteria under different C/N ratio constraints: quantitative molecular mechanism and microbial community dynamics†

Duntao Shu,^{‡ab} Yanling He,^{*c} Hong Yue,^{‡d} Junling Gao,^e Qingyi Wang^e
and Shucheng Yang^f

The anaerobic ammonium oxidation (anammox) process has mainly been applied to NH_4^+ -N-rich wastewater with very low levels of organic carbon (<0.5 g COD per g N). Some anammox bacteria species have the capacity to oxidize organic carbon with nitrate as the electron acceptor. However, little is known about the organotrophic anammox nature of "*Ca. Brocadia sinica*". To elucidate the metabolic versatility and microbial succession of "*Ca. Brocadia sinica*" under TOC/TN stress conditions, the influence of TOC/TN ratios on the nitrogen transformation pathway and the dynamics of microbial communities were investigated. It was found that an appropriate TOC/TN ratio (<0.2) could promote the anammox activity over the short-term. Meanwhile, "*Ca. Brocadia sinica*" had higher tolerance to higher TOC/TN (>0.4) abiotic stresses. Mass balance indicated that organotrophic anammox could outcompete denitrifiers under a TOC/TN ratio of 0.1–0.2. Quantitative response relationships and pathway analysis revealed that (AOA *amoA* + AOB *amoA* + *anammox* + *nrfA*)/bacteria, *nrfA*/(*narG* + *napA*), and *nrfA* were the key functional gene groups determining the organotrophic anammox contribution. Additionally, MiSeq sequencing showed that *Planctomycetes*, *Proteobacteria*, *Chloroflexi*, and *Chlorobi* were the most abundant phyla in the organotrophic anammox system. Furthermore, higher TOC/TN ratios (>0.40) could result in the community succession of anammox species, in which "*Ca. Jettenia caeni*" and "*Ca. Kuenenia stuttgartiensis*" were the dominant organotrophic anammox bacteria species. Overall, combined analyses revealed that the coupling of anammox, DNRA (organotrophic anammox), and denitrification comprised the primary pathway that accounted for TOC and nitrogen removal.

Received 15th February 2016
Accepted 5th September 2016

DOI: 10.1039/c6ra04114k

www.rsc.org/advances

1. Introduction

Anaerobic ammonium-oxidizing (anammox) bacteria, which were discovered in a denitrifying bioreactor and mediated by

Planctomycete bacteria,^{1,2} have the unique ability to combine ammonium and nitrite to form N_2 . Understanding of the microbial nitrogen cycle has therefore been fundamentally altered by the discovery of anammox bacteria.³ The anammox-related process, which is a lithoautotrophic nitrogen removal process, has been successfully applied in the treatment of ammonia-rich wastewater with low COD (chemical oxygen demand): N (nitrogen) ratios due to its cost-effective and energy-efficient qualities.^{4,5}

Nevertheless, the slow growth rate, low cell yield, and sensitivity to environmental conditions which characterize anammox bacteria have presented major obstacles to the broader application of anammox-related processes. For instance, in a mainstream and side-stream nitrogen removal process, anammox bacteria were unable to avoid the influences of volatile fatty acids (VFA) (expressed as total organic carbon), which existed in large volume in municipal and industrial WWTPs.⁶ Although the addition of organic matter had significant effects on anammox bacteria in many studies, there has been no consensus on which TOC (total organic carbon) to TN (total nitrogen) ratios inhibit/or affect the anammox bacteria.^{7–9}

^aState Key Laboratory of Crop Stress Biology in Arid Areas, College of Life Sciences, Northwest A&F University, Yangling, Shaanxi 712100, China

^bCenter for Mitochondrial Biology and Medicine, The Key Laboratory of Biomedical Information Engineering of the Ministry of Education, School of Life Science and Technology, Xi'an Jiaotong University, Shaanxi 710049, China

^cSchool of Human Settlements & Civil Engineering, Xi'an Jiaotong University, Shaanxi 710049, China. E-mail: heyl@mail.xjtu.edu.cn; Fax: +86 029 83395128; Tel: +86 029 83395128

^dState Key Laboratory of Crop Stress Biology in Arid Areas, College of Agronomy and Yangling Branch of China Wheat Improvement Center, Northwest A&F University, Yangling, Shaanxi 712100, China

^eSchool of Chemical Engineering & Technology, Xi'an Jiaotong University, Shaanxi 710049, China

^fSchool of Energy and Power Engineering, Xi'an Jiaotong University, Shaanxi 710049, China

† Electronic supplementary information (ESI) available. See DOI: 10.1039/c6ra04114k

‡ These authors contributed equally to this work.

In addition, investigations have reported that the most critical point in the competition between autotrophic anammox, organotrophic anammox, and heterotrophic denitrification for TOC is the C : N ratio in the influent.^{10,11} Moreover, detailed evidence describing the contribution of organotrophic or mixotrophic anammox processes to nitrogen removal in the presence of TOC has yet to be presented.

To date, six anammox bacteria genera have been detected and proposed using 16S and 23S rRNA gene sequencing: “*Ca. Brocadia sinica*”, “*Ca. Anammoxoglobus propionicus*”, “*Ca. Jettenia caeni*”, “*Ca. Kuenenia stuttgartiensis*”, “*Ca. Scalindua* sp.”, and “*Ca. Brocadia anammoxidans*”.^{12,13} A few recent studies^{10,14,15} have reported that some anammox bacteria species, including *Ca. Jettenia asiatica*, *Ca. Ananimoxoglobus propionicus*, *Ca. Brocadia fulgida*, and *Ca. Kuenenia stuttgartiensis* have the capacity to oxidize acetate and propionate. In addition, phylogenetic classification of anammox 16S rRNA¹² revealed that “*Ca. Brocadia sinica*” was closely related to the group “*Ca. Brocadia Scalindua* sp.” and “*Ca. Brocadia anammoxidans*”, which were organotrophic. Thus, it could be speculated that TOC might have been utilized as electron donors by “*Ca. Brocadia sinica*” and this phylum could success to other organotrophic anammox species. However, whether the organotrophic nature of “*Ca. Brocadia sinica*” participated in TOC oxidation remains unverified. This inspired us to explore the adaptability and organotrophic nature of “*Ca. Brocadia sinica*” in the presence of TOC.

In addition, anammox sludge in wastewater treatment plants is a highly complex system of eukaryotes (protozoa, fungi, and microalgae),^{16–19} bacteria, archaea, and viruses, in which bacteria are dominant. Molecular biological methods which have been applied to explore the microbial structures in anammox-related system include clone library of 16S rRNA genes, denaturing gradient gel electrophoreses (DGGE) analysis and fluorescence *in situ* hybridization (FISH). With the recent rapid development of the next-generation sequencing, high-throughput sequencing has been received more attention. 454 pyrosequencing²⁰ and Illumina high-throughput sequencing²¹ have been applied to the investigation of microbial communities in lab-scale and pilot-scale anammox-related systems. However, little is known about the dynamics of microbial communities and functional genes under TOC/TN constraints. Knowledge of microbial community structures and the links to different TOC stresses is therefore essential for understanding the profile of the organotrophic anammox process.

Furthermore, nitrification, denitrification, and anammox could co-exist in anammox-related systems when the TOC was present.²² These nitrogen removal processes involve several functional genes which have played key roles in microbial nitrogen cycling, including anammox 16S rRNA, archaea ammonia monooxygenase (AOA-*amoA*), ammonia monooxygenase (AOB-*amoA*), nitrite oxidoreductase (*nrxA*), periplasmic nitrate reductase (*napA*), membrane-bound nitrate reductase (*narG*), dissimilatory nitrate reductase (*nrfA*), copper-containing nitrite reductase (*nirK*), nitrite reductase (*nirS*), and nitrous oxide reductase (*nosZ*).^{23,24} Nevertheless, the quantitative response relationship between nitrogen transformation rates and functional genes are unknown in the anammox system. Furthermore, the corresponding

dynamics of microbial community structures and functional gene groups on the quantitative molecular level in the organotrophic anammox process are still unclear.

The present study is the first to systematically investigate the microbial community structure dynamics and quantitative molecular mechanisms of nitrogen transformation in anammox systems under different TOC stress constraints. Based on these arguments, this study was performed for the following purposes: (1) to assess the impacts of different TOC/TN ratios on organotrophic anammox growth rates and activity using batch experiments; (2) to evaluate the long-term adaptation of “*Ca. Brocadia sinica*” and contribution of organotrophic anammox bacteria species under different TOC/TN constraints; (3) to explore the quantitative response relationships between nitrogen transformation rates and functional gene groups, and (4) to investigate the dynamics of nitrogen-related microbial communities under TOC/TN stress conditions.

2. Methods

2.1. Kinetic evaluation and treatment performance of an anammox bioreactor under different TOC/TN ratio constraints

The anammox biomass used in this study was taken from a laboratory-scale sequencing batch reactor (SBR) with a working volume of 2.6 L. The anammox-SBR system has been operated for over 18 months under mesophilic conditions (35 ± 2 °C) with hydraulic residence time (HRT), influent NH₄⁺-N, and NO₂[−]-N concentrations of 4 h, 200 mg L^{−1} and 220 mg L^{−1}, respectively. According to Shu *et al.*,²¹ the “*Ca. Brocadia sinica*” phylum comprised the dominant anammox bacteria in this SBR system. Prior to the addition of TOC, the stock solution of organic carbon sources was prepared by mixing it with acetate and propionate at a volume ratio of 1 : 1. In the case of batch experiments, 10 mL of anammox biomass were dispensed into 60 mL of liquid in 100 mL serum vials with different TOC/TN ratios of 0, 0.05, 0.10, 0.20, 0.41, 0.61, and 0.82 (Table 1). Finally, the concentration values of mixed liquor volatile suspended solids (MLVSS), NH₄⁺-N and NO₂[−]-N in each vial were 2850 mg L^{−1}, 80 mg L^{−1}, and 96 mg L^{−1}, respectively. The above experimental procedures were performed in an anaerobic glove box. All the experimental vials were thereafter incubated at 32 °C and shaken at a speed of 120 rpm in the dark. The water samples for further kinetic analysis were taken from the vials hourly over 8 hours.

To investigate the effects of different TOC/TN ratios on “*Ca. Brocadia sinica*”, the specific anammox activity (SAA) and specific anammox growth rates (μ_{AN}) were measured according to the following models.²⁵

$$SAA = \frac{SAA_{\max}}{1 + \frac{K_S}{S} + \frac{S}{K_I}} \quad \text{and} \quad \mu_{AN} = \frac{\mu_{AN\max}}{1 + \frac{K_S}{S} + \frac{S}{K_I}} \quad (1)$$

where K_S is the half saturation constant; S is the TOC concentration; K_I is the inhibition constant; and SAA_{\max} and $\mu_{AN\max}$ are the maximum specific anammox activity and specific anammox growth rates, respectively.

Table 1 Short- and long-term experiment conditions

	NH ₄ ⁺ -N (mg L ⁻¹)	NO ₂ ⁻ -N (mg L ⁻¹)	TOC (mg L ⁻¹)	TOC : TN
Batch experiments				
Batch test 1	80	96	—	—
Batch test 2	80	96	8.99	0.05
Batch test 3	80	96	17.98	0.10
Batch test 4	80	96	35.96	0.20
Batch test 5	80	96	71.91	0.41
Batch test 6	80	96	107.87	0.61
Batch test 7	80	96	143.82	0.82
Long-term experiments				
Phase I (1–62 days)	190	220	—	—
Phase II (63–79 days)	190	220	41.20	0.10
Phase III (80–95 days)	190	220	82.40	0.20
Phase IV (96–106 days)	190	220	164.79	0.40
Phase V (107–120 days)	190	220	329.59	0.80
Recovery (121–140 days)	70	84	—	—

For long-term experiments, ~900 mL of seeding sludge were derived from the initial SBR system and then cultivated in a new SBR system with a working volume of 2.6 L. The new SBR system was operated under the same mesophilic conditions with mineral medium and trace element solution.¹ The new anammox-SBR system was run in a 12 hour-cycle and fed with 190 mg L⁻¹ NH₄⁺-N and 220 mg L⁻¹ NO₂⁻-N. Because the anammox bacteria tolerate to lower DO concentrations (<0.5 mg L⁻¹) well and the dissolved oxygen (DO) in anammox-SBR system was consumed by some of the aerobic bacteria, the dissolved oxygen (DO) was not controlled in the anammox-SBR system. More specifically, the dissolved oxygen (DO) was not controlled in any of the phases, and it measured 1.0–1.3 mg L⁻¹ in the influent and 0.08–0.3 mg L⁻¹ in the effluent. After the adaptation stage, the experimental batches with different ratios of TOC/TN had values of 7.2 mL, 14.4 mL, 28.8 mL, and 57.6 mL (7.24 g TOC per L) mixed solution of sodium acetate and propionate. These were added into the reactor automatically at the end of each feeding period to maintain influent TOC/TN ratios of 0.10, 0.20, 0.40, and 0.80 (Table 1).

2.2. DNA extraction, PCR amplification and Illumina MiSeq sequencing

After a start-up period, ~0.5 g of anammox biomass was collected from the SBR system at the end of each phase. Then genomic DNA was extracted by using the FastDNA® SPIN Kit for Soil (Mp Biomedicals, Illkirch, France) according to the manufacturer's protocols. DNA purity was checked in agarose gel (1.2%) and its concentration was determined with Nanodrop Spectrophotometer ND-1000 (Thermo Fisher Scientific, USA).

Before sequencing, genomic DNA was amplified by PCR using primer sets 338F (5'-barcode-ACTCCTACGGGAGGCAG-CAG-3') and 806R (5'-barcode-GGACTACHVGGGTWTCTAAT-3') for the V3–V4 regions of the bacterial 16S rRNA. The amplification reactions were performed in triplicate using the previously described primers and protocols.²⁶ After amplification, the PCR products were purified with the AxyPrep DNA

Gel Extraction Kit (Axgen, USA) and quantified with a QuantiFluor™-ST (Promega, USA) according to the instructions. Then the three individual PCR products were pooled in equimolar ratios and amplicon libraries were constructed before sequencing. Finally, the amplicon libraries were prepared and then run on the MiSeq Illumina platform (Shanghai Personal Biotechnology Co., Ltd, Shanghai, China). All the raw sequences have been deposited into the National Center for Biotechnology Information (NCBI) Sequence Read Archive (SRA) database (Accession number: SRR2962328).

2.3. Sequence processing and bioinformatics analysis

Following sequencing, all the raw reads were initially merged using FLASH (Version 1.2.11, <http://ccb.jhu.edu/software/FLASH/>) software, and then Trimmomatic (Version 0.33, <http://www.usadellab.org/cms/?page=trimmomatic>) was used to remove barcodes, primers, and low quality reads. After filtration, the remaining set of effective sequences were clustered into operational taxonomic units (OTUs) using Usearch (Version 8.1, <http://drive5.com/uparse/>) at a 97% similarity setting. Then, the taxonomy was assigned using an RDP classifier (Version 2.2, <http://sourceforge.net/projects/rdp-classifier/>) via Silva SSU database (Release 119, <http://www.arb-silva.de>) with a set confidence threshold of 70%. Furthermore, appropriate subsample depth analyzing was conducted to avoid unequal sampling depth biases during comparison of microbial diversity and to ensure adequate sample depth while retaining the lowest sequences.²⁷ Subsequently, alpha diversity statistics including Chao 1 estimator, ACE estimator, Shannon index, Simpson index, Good's coverage, and rarefaction curves at a distance of 0.03 (equivalent to 97% similarity), were calculated for five samples using the Mothur program (Version 1.30.1, http://www.mothur.org/wiki/Main_Page).²⁸ On the basis of the UniFrac metric, beta diversity statistics including cluster analysis (CA), (un)weighted UniFrac distance metrics, and principal co-ordinates analysis (PCoA) were also conducted to evaluate the similarities and differences of five samples.

2.4. Quantitative real-time PCR

Compared with RNA-based techniques, DNA-based methods are more robust alternative for measuring the total microbial growth rates and activity for the given environmental conditions because they account for all active, dormant, and deceased cells.²⁹ Thus, quantitative real-time PCR, a DNA-based technology, was used to explore the “key players” in the nitrogen removal process and its quantitative molecular mechanism. The absolute abundance of bacteria 16S rRNA, anammox 16S rRNA, *AOB amoA*, *AOA amoA*, *nosZ*, *nirS*, *nirK*, *narG*, *napA*, and *nrfA* were quantified in triplicate by Mastercycler ep realplex (Eppendorf, Hamburg, Germany) based on the SYBR Green II method using the described primers and protocols.²⁶ The plasmids containing bacteria 16S rRNAs, anammox bacteria 16S rRNAs, *Nitrobacter* 16S rRNAs, *Nitrospira* 16S rRNAs and other functional genes (*i.e.* *amoA*, *nosZ*, *nirS*, *nirK*, *narG*, *napA*, *nrfA*, *mcrA*, *dsrA*) were manufactured by Sangon Biological Technology Company (Sangon Biological Engineering Co., China).

To generate the standard curve, plasmid DNAs were diluted to yield a series of concentrations, each with a 10-fold difference. The efficiencies of the qPCR assays ranged from 102% to 110%, and the R^2 value for each standard curve line exceeded 0.98. The C_t value (threshold cycle) was determined to quantify the copy number of all of the above mentioned genes. The qPCR amplification was conducted in 10 μ L reaction mixtures, consisting of 5 μ L SYBR® Premix Ex Taq™ II (Takara, Japan), 0.25 μ L of each primer, 1 μ L of genomic DNA and 3.5 μ L dd H₂O. The primers and qPCR protocols followed Shu *et al.*²¹ Each qPCR reaction was run in triplicate.

2.5. Statistical analysis

Analytical measurements of NH_4^+ -N, NO_2^- -N, NO_3^- -N, TN, and TOC in influent and effluent wastewater in the anammox bioreactor were performed according to the standard methods.³⁰ The specific anammox activity and growth rates were measured, and the kinetic parameters were fitted using the secant method embedded in AQUASIM 2.1d.³¹

The ecological association between rates of nitrogen transformation and functional gene groups were evaluated *via* stepwise regression analyses (SPSS 20, USA). Furthermore, the direct and indirect contribution of different functional gene groups on nitrogen transformation rates were determined using path analysis according to the methods described by Pang *et al.*³² Values of direct effects (path coefficients)³³ were derived by the simultaneous solution of the normal equations for multiple linear regression using SPSS Statistics 20 (IBM, USA). Indirect effects were obtained from simple correlation coefficients between functional genes using SPSS Statistics 20 (IBM, USA) (<http://www-01.ibm.com/software/analytics/spss/>).³²

3. Results and discussion

3.1. Short-term experiments and kinetics evaluation

To explore the specific anammox growth activity (SAA) and anammox growth rates (μ_{AN}) in eight batch tests at different TOC/TN ratios, the rates of NH_4^+ -N consumption were measured and the kinetics were fitted according to the AQUASIM 2.1d.³¹ As shown in Fig. 1, the kinetics matched well with the corresponding experimental measurements. Generally speaking, with increased ratios of TOC/TN from 0.05 to 0.20, the evaluated μ_{AN} increased from 0.1093 d^{-1} to 0.1236 d^{-1} (Fig. 1a–c). The results revealed that appropriate TOC/TN ratios could improve the anammox activity. However, the μ_{AN} declined from 0.1183 d^{-1} to 0.0926 d^{-1} when the TOC/TN ratios were increased from 0.41 to 0.82 (Fig. 1d–f). Compared with batch test 1 (0.1102 d^{-1}), the results indicated that the maximum μ_{AN} ($\mu_{\text{AN max}}$) was 0.1236 d^{-1} in the presence of a TOC/TN ratio of 0.20, which was 10.8% higher than that observed in batch test 1. In addition, the μ_{AN} in batch test 5 and batch test 6 were also higher than batch test 1. Therefore, these results indicated that “*Ca. Brocadia sinica*” have tolerance to higher TOC stress conditions (TOC/TN > 0.20).

Additionally, the dependence of SAA and μ_{AN} on the different TOC/TN stresses were well described by the substrate inhibition

kinetics model. The results from Fig. 1g–h showed that $0.0524 \text{ kg N per kg VSS per d}$ and 0.1356 d^{-1} were the maximum SAA (SAA_{max}) and $\mu_{\text{AN max}}$, respectively. The inhibition constants of nitrite and TOC were $4.8651 \text{ mmol L}^{-1}$ (122 mg N per L) and $2.4762 \text{ mmol L}^{-1}$ ($196 \text{ mg L}^{-1} \text{ TOC}$), respectively. Meanwhile, the 95% confidence interval showed in Fig. 1g and h further indicate that the specific anammox growth rate under TOC/TN abiotic stresses could be described by eqn (1).

Kartal *et al.* found “*Ca. Kuenenia stuttgartiensis*” have the unique ability to use TOC as electron donors to reduce the nitrate and nitrite to ammonium.³⁴ Winkler *et al.* also found that both “*Ca. Brocadia fulgida*” and “*Ca. Anammoxoglobus propionicus*” were capable of oxidizing VFAs.¹⁰ Moreover, it was found that the appropriate influent C/N ratio for this process is $0.5 \text{ g COD per g NH}_4^+$ -N. Huang *et al.* found that “*Ca. Jettenia asiatica*” have an organotrophic anammox nature and that they could obtain high rates of NH_4^+ -N conversion at low COD : N ratios (<1.5).¹⁴ In addition, Du *et al.* found that anammox bacteria could outcompete heterotrophic denitrifiers. In this study, “*Ca. Brocadia sinica*” have higher rates of specific anammox growth and activity at TOC/TN ratios ranging from 0.05 to 0.61. There are two possible explanations for this result. One is that “*Ca. Brocadia sinica*” oxidized the TOC to CO_2 with nitrate and/or nitrite as the electron acceptor; the other is that the surplus TOC were consumed by heterotrophic microorganisms. These two possible explanations demanded exploration and either rejection or confirmation based on detailed evidence from long-term treatment performance and mass balance.

3.2. Treatment performance of organotrophic anammox and mass balance at different TOC/TN ratios

In order to evaluate the treatment profiles of the organotrophic anammox process for nitrogen and TOC removal, a long-term experiment was carried out over 140 days. As shown in Fig. 2, experiment was performed without the addition of TOC in phase I (1–62 days). During the phase I, the respective NH_4^+ -N, NO_2^- -N, and total nitrogen removal (TN) efficiencies were $96.19 \pm 2.52\%$, $99.85 \pm 0.46\%$, and $89.62 \pm 1.94\%$, respectively. Correspondingly, NH_4^+ -N, NO_2^- -N, and TN nitrogen transformation rates reached at 0.36 ± 0.01 , 0.45 ± 0.01 , and $0.74 \pm 0.02 \text{ kg N per m}^3 \text{ per d}$. The stoichiometric ratio of NH_4^+ -N, NO_2^- -N, and NO_3^- -N were $1 : (1.24 \pm 0.04) : (0.20 \pm 0.03)$, which was accordant with the theoretical values for the anammox process.¹ During phase II (63–79 days), the NH_4^+ -N removal efficiencies slightly declined to $93.28 \pm 3.17\%$ (Fig. 2). However, NO_2^- -N and TN efficiencies increased to 100% and $92.01 \pm 2.81\%$. The NH_4^+ -N, NO_2^- -N, and TN transformation rates were 0.35 ± 0.01 , 0.45 ± 0.02 , and $0.76 \pm 0.03 \text{ kg N per m}^3 \text{ per d}$, respectively (Fig. 2). Nevertheless, the stoichiometric ratios of NH_4^+ -N, NO_2^- -N, and NO_3^- -N were changed to $1 : (1.31 \pm 0.07) : (0.12 \pm 0.05)$. During phase III (80–95 days), the NO_2^- -N and TN removal efficiencies did not vary significantly. However, the NH_4^+ -N removal efficiency decreased to $88.17 \pm 2.78\%$. In addition, the NH_4^+ -N transformation rates decreased to $0.33 \pm 0.01 \text{ kg N per m}^3 \text{ per d}$. During phase IV (96–

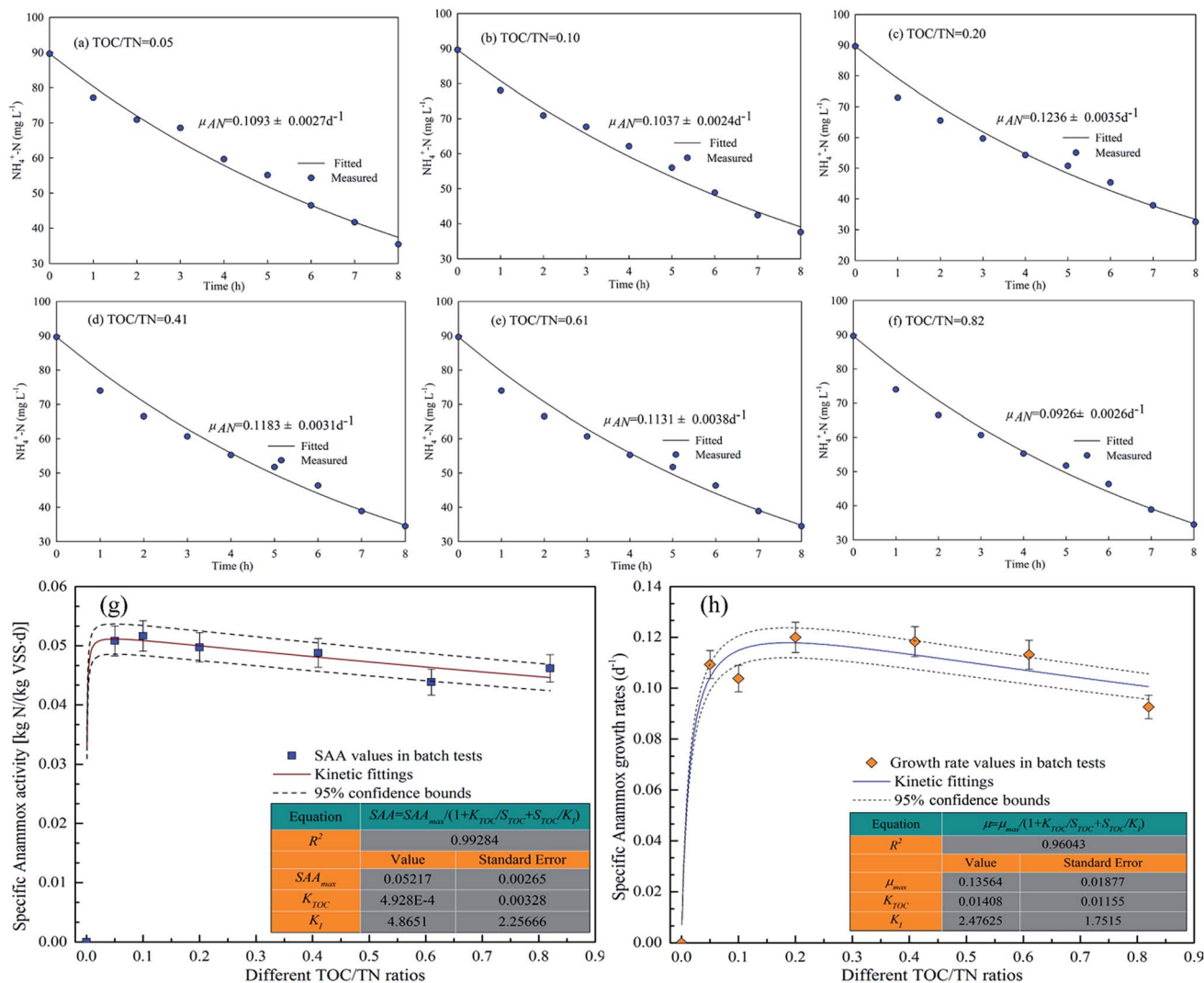


Fig. 1 (a)–(f) The kinetic fitted and measured $\text{NH}_4^+\text{-N}$ consumption profiles in six 8 h batch tests under different TOC/TN ratios; (g) the actually observed and model-fitted relationships between TOC/TN ratios and specific anammox activity using substrate inhibition kinetics; (h) relationships between TOC/TN ratios and specific anammox growth rates.

106 days), the $\text{NH}_4^+\text{-N}$ and TN removal efficiencies dropped to $70.75 \pm 10.98\%$ and $86.85 \pm 5.02\%$, respectively. The $\text{NH}_4^+\text{-N}$ transformation rates further decreased to (0.26 ± 0.04) kg N per m^3 per d. During phase V (96–106 days), the effluent $\text{NH}_4^+\text{-N}$ levels increased remarkably and the $\text{NH}_4^+\text{-N}$ and TN removal efficiencies decreased sharply to $10.23 \pm 6.74\%$ and $60.23 \pm 3.34\%$, respectively. In the recovery phase (120–140 days), the operational strategy without TOC was performed. Because the anammox was seriously suppressed under high TOC/TN stress, the influent $\text{NH}_4^+\text{-N}$ and $\text{NO}_2^-\text{-N}$ levels were set at 70 and 84 mg L^{-1} , respectively. Meanwhile, 10 mL high-loaded anammox sludge from another anammox reactor was added at the beginning of day 125.³⁵ The results from Fig. 2a indicate that this type of high-loaded sludge could be beneficial for the rapid recovery of anammox activity.

In general, the results from the long-term treatment performance of assessment of the organotrophic anammox system under different TOC/TN ratio conditions indicated that

the autotrophic anammox process was the primary process accounting for nitrogen removal in phases I–III, which was consistent with the results from the short-term experiment in this study as well as the work of Tang *et al.*⁹ In addition, due to the weakening of the anammox process in phase IV, the decreased production of $\text{NO}_3^-\text{-N}$ indicated that organotrophic anammox and heterotrophic denitrifiers could coexist for purposes of nitrogen removal. There are two reasons which may explain these results: (1) organotrophic anammox bacteria could consume the acetate and propionate to reduce the nitrate and nitrite to ammonia;^{11,34} (2) heterotrophic denitrification and denitritation could contribute to the TN removal.

The severely inhibited anammox in phase V along with increased $\text{NH}_4^+\text{-N}$ concentration and further decreased $\text{NO}_3^-\text{-N}$ effluent production indicate that autotrophic anammox could not outcompete heterotrophic microorganisms under high TOC/TN ratios. Moreover, it was found that lower ratios of TOC/

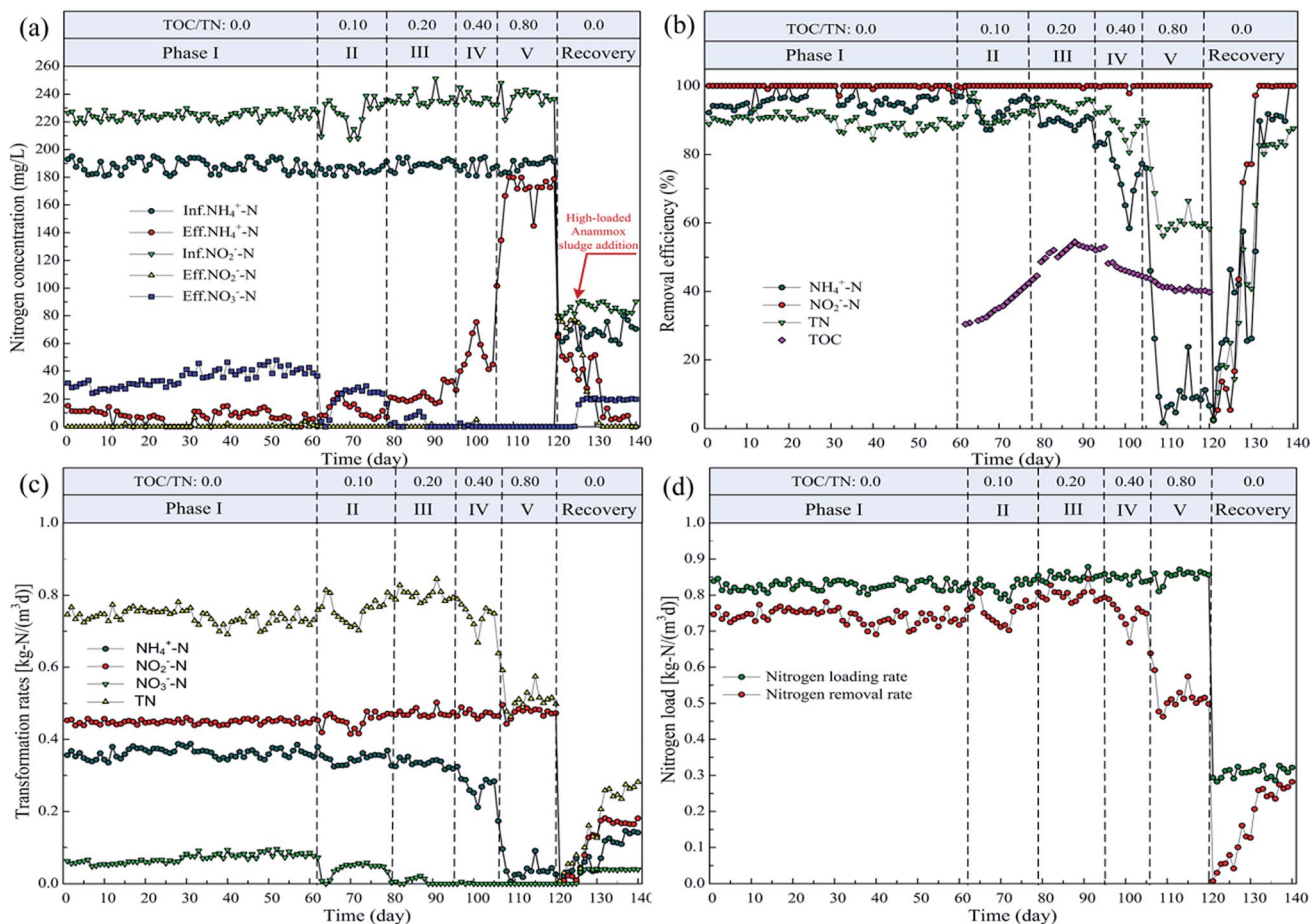


Fig. 2 Long-term performance of anammox-SBR system under different TOC/TN ratio stresses. (a) Nitrogen concentration; (b) nitrogen removal efficiency; (c) nitrogen transformation rates; (d) nitrogen load.

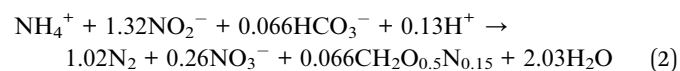
TN (<0.2) were useful for simultaneous removal of nitrogen and TOC but anammox growth rates were suppressed by higher TOC/TN ratios (>0.40).

Based on the above results, it could be seen that the average NO_3^- -N production was $35.37 \pm 6.18 \text{ mg L}^{-1}$ without the addition of acetate and propionate in phase I, which was very close to the theoretical production. However, during phases II–V, the average nitrate production was far less than that in phase I. For instance, the average nitrate production was 20.32 mg L^{-1} in phase II. Ahn *et al.*³⁶ have reported that 1 g nitrate would be reduced when 3.31 g chemical oxygen demand (COD) was consumed. Thus, 15.05 mg ($35.37 - 20.32 = 15.05$) nitrate would be reduced in another pathway when 49.82 mg COD ($15.05 \times 3.31 = 49.82$) was consumed. In phase II, the TOC/TN ratio was 0.19 (equal to 110 mg L^{-1} COD) and the TOC removal efficiency was $36.65 \pm 4.56\%$, revealing that 40.32 mg L^{-1} was consumed in phase II. It is obvious that nitrate was in too short a supply to foster denitrification in phases III–V. It can be concluded that organotrophic anammox bacteria which consumed TOC and thus reduced the levels of nitrate existed in phases II–V.³⁷

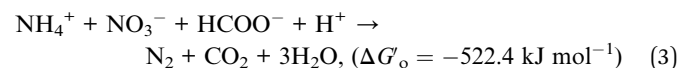
Some studies have reported a total of four possible nitrogen and TOC consumption processes: the autotrophic anammox

process eqn (2); the organotrophic anammox process eqn (3); the denitrification process eqn (4); and the denitrification process eqn (5).^{5,12,38} To further understanding the nitrogen pathway in the organotrophic anammox process, the removal of NH_4^+ -N, NO_2^- -N, NO_3^- -N, and TOC were calculated based on nitrogen, TOC mass balance and eqn (2)–(5).

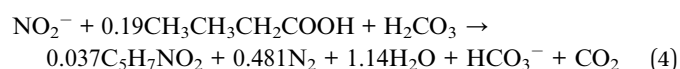
Autotrophic anammox:



Organotrophic anammox:



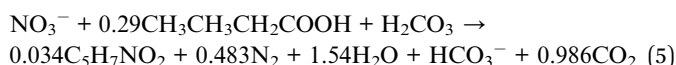
Denitrification:



Denitrification:

Table 2 Contribution of different pathways to nitrogen removal on the basis of COD (Chemical oxygen demand) and nitrogen mass balance at different TOC/TN ratios

Consumption	Removal route	Phase II	Phase III	Phase IV	Phase V
NH_4^+ -N removal (mg L^{-1})	Anammox (autotrophic)	150.19	135.96	116.91	7.84
	Anammox (organotrophic)	22.87	30.04	15.53	11.46
NO_2^- -N removal (mg L^{-1})	Anammox (autotrophic)	198.25	179.47	154.32	10.35
	Denitrification	27.73	46.51	71.66	215.63
NO_3^- -N removal (mg L^{-1})	Anammox (organotrophic)	22.87	30.04	15.53	11.46
	Denitrification	—	—	—	—
Biomass increased (mg N)	Anammox (autotrophic)	9.91	8.97	7.72	0.52
	Anammox (organotrophic)	0.75	0.99	0.51	0.38
	Denitrification	1.03	1.72	2.65	7.98
Total biomass increased (mg N)	—	11.69	11.69	10.88	8.87
Total nitrogen removal (mg L^{-1})	—	378.72	400.27	367.5	256.95
Average percentage of nitrogen removal routes (%)	Anammox (autotrophic)	76.03	69.06	67.48	2.42
	Anammox (organotrophic)	11.88	14.76	8.31	8.77
	Denitrification	7.05	11.19	18.78	80.81
	Denitrification	—	—	—	—
	Other pathways	5.04	4.99	5.43	7.99



As shown in Table 2, during phases II–V of the organotrophic anammox, only a small contribution to the overall nitrogen removal was made. In general, as the TOC/TN ratio increased from 0.10 to 0.80, the average nitrogen removal pathway percentage observed in the autotrophic anammox process decreased from 76.03% (phase II) to 2.42% (phase V). Correspondingly, the heterotrophic denitrification contribution increased from 7.05% (phase II) to 80.81% (phase V). These results indicate that autotrophic anammox and organotrophic anammox could not outcompete heterotrophic denitrification at high TOC/TN ratios. This was because the growth rate of the heterotrophic denitrification process enjoys have much shorter doubling times (2–16 hours), which renders the overall growth rate higher than that of anammox bacteria (8–12 days).¹²

Although the TOC/TN ratios were further increased, the organotrophic anammox contribution rates of 11.88%, 14.76%, 8.31%, and 8.77%, respectively, did not vary significantly. Interestingly, the maximum organotrophic anammox contribution was achieved at the TOC/TN ratio of 0.20. These results indicated that the organotrophic anammox activity had been maximized in this TOC/TN ratio. Meanwhile, the organotrophic anammox could outcompete heterotrophic denitrification in phases II–III. The reason for these favorable results is that organotrophic anammox could utilize nitrate and nitrite as electron acceptors to oxidized acetate and propionate under these conditions. Other nitrogen pathways such as fermentation and sulfur-based autotrophic denitrification varied from 5.04% to 7.99%.⁷

3.3. Quantification of nitrogen-related 16S rRNA and functional genes

In order to gain insight into the variation of nitrogen-related functional genes under TOC/TN stress conditions, samples of anammox biomass were taken from the end of each phase and

the copy numbers of all above mentioned 16S rRNA and functional genes were quantified. As shown in Fig. 3a–f, the gene copy numbers of bacterial 16S rRNAs were in the same order of magnitude in phases I–V. The gene copy numbers of anammox 16S rRNAs were also in the same order of magnitude ranging from 2.50×10^8 to 4.07×10^8 copies per g wet sludge even though the anammox were severely suppressed, indicating that the abundance of anammox had no remarkable reduction in the system, which was consistent with the finding of Du *et al.*²³ It was evident that higher TOC/TN ratios (>0.40) could result in the community succession of anammox species in this study.

The copy numbers of three nitrification groups, including AOA *amoA*, AOB *amoA* and *nrrA* genes, were summarized in Fig. 3b. With the increase in TOC/TN ratios from 0–0.40 during phases I–IV, the absolute abundance of AOB *amoA* and *nrrA* gradually increased from 1.66×10^6 to 1.18×10^7 copies per g wet sludge, 4.87×10^4 to 1.04×10^5 copies per g wet sludge, respectively. However, higher TOC/TN ratios in phase V had adverse effects on these two genes, suggesting that the activity of AOB and NOB (nitrite oxidizing bacteria) have tolerate to TOC/TN ratios of 0.1–0.4 well. In addition, the absolute abundance of AOA *amoA* increased from 1.11×10^2 to 1.21×10^2 copies per g wet sludge in phases III–V, suggesting that AOA had positive relationship with TOC. The results indicated that AOA might have an organotrophic nature, which was consistent with the work of Mußmann *et al.*³⁹

As illustrated in Fig. 3c, the dissimilatory nitrogen reduction gene *nrfA* increased from 2.02×10^4 to 6.95×10^5 copies per g wet sludge during phases I–V as the TOC/TN ratios increased. Kartal *et al.* found that some anammox bacteria species could engage in “disguised denitrification” in the form of the reduction of nitrate and nitrite (termed DNRA).³⁴ As depicted in Fig. 3f, the variation of *nrfA*/anammox and anammox/bacteria had a high degree of consistency, indicating that DNRA or organotrophic anammox had greatly contributed to nitrogen removal in the organotrophic anammox process. In addition, Fig. 3c indicated that the absolute gene abundance of *napA* increased in phases I–IV, while it decreased in phase V. As

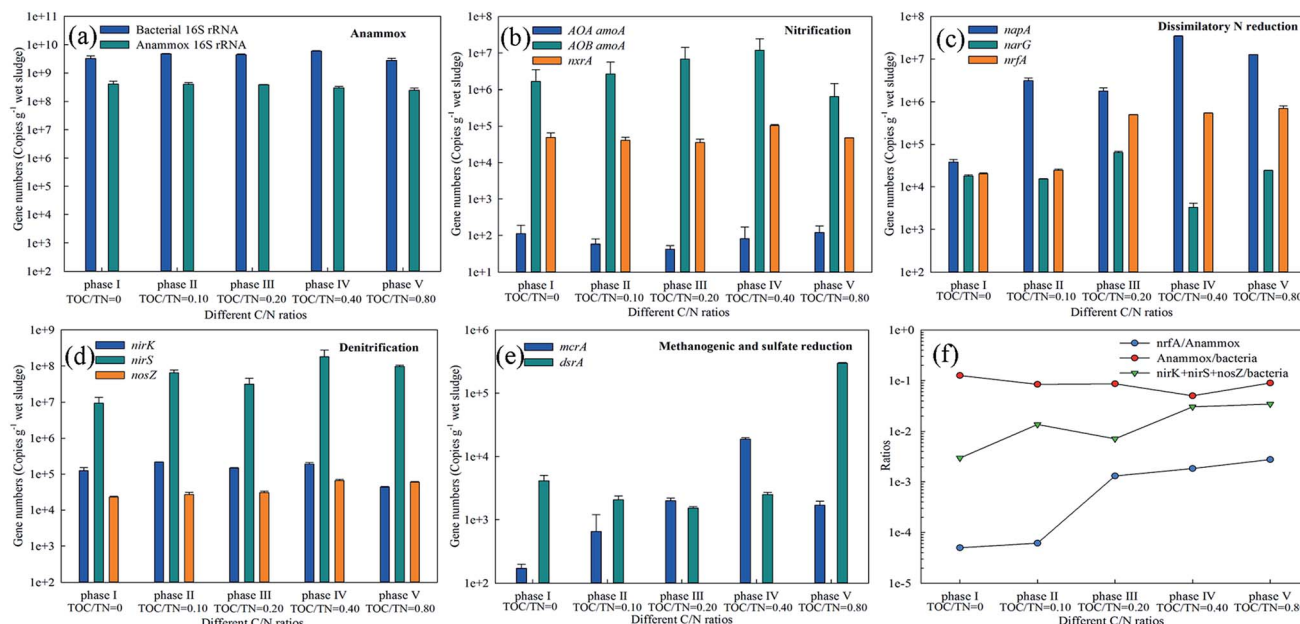


Fig. 3 Absolute abundance of microbial communities and functional genes in the anammox-SBR system. (a) Total bacterial and anammox bacterial 16S rRNA; (b) AOA *amoA*, AOB *amoA*, and *nxrA*; (c) *napA*, *narG*, and *nrfA*; (d) *nirK*, *nirS*, and *nosZ*; (e) *mcrA* and *dsrA*; (f) ratios of different functional gene groups. Error bars represent standard deviation calculated from three independent experiments.

compared to the *napA* gene, the absolute gene abundance of the *narG* gene in phases I–III was nearly one to two orders of magnitude higher than in phases IV–V. The conversion of $\text{NO}_3^- \rightarrow \text{NO}_2^-$ is catalyzed by the *napA* and *narG* genes. Therefore, the results indicated that high TOC/TN ratios in phase IV–V had no significant influence on the rates of NO_3^- -N reduction.

As shown in Fig. 3d, the absolute abundance of *nirS* in phase IV was nearly one order of magnitude greater than other four phases. The absolute abundance of the *nirK* gene in phases I–IV was nearly the same order of magnitude, while it slightly decreased in phase V. The absolute abundance of the *nosZ* gene increased from 2.28×10^4 to 6.59×10^5 copies per g wet sludge during phases I–V as the TOC/TN ratios increased. These results showed that the absolute abundance of denitrification genes did not vary dramatically, suggesting that denitrification was not dominant process accounting for nitrogen removal under the different TOC/TN stress conditions; this was accordant with the results of Table 2.

Furthermore, as shown in Fig. 3e, the absolute abundance of the *mcrA* gene increased gradually during phases I–IV, while it decreased in phase V. In terms of the *dsrA* gene, copy numbers increased from 4.14×10^3 to 2.98×10^5 copies per g wet sludge. Notably, as illustrated in phases IV–V, methanogens could compete with sulfate reduction bacteria for the TOC.

Taken together, it is plausible that the co-existence of autotrophic anammox, organotrophic anammox (or DNRA), and denitrification were the primary pathway that accounted for nitrogen removal under TOC/TN stress conditions.

3.4. Functional gene groups determining nitrogen transformation rates

In this study, single functional genes and functional gene group ratios were used as input variables and introduced into stepwise

regression analyses. Results showed nitrogen transformation in phases I–II differed from that in phases III–V. Therefore, the key functional groups in phases I–II and in phases III–V were separately investigated to characterize the nitrogen transformation pathway under different TOC/TN stress conditions.

As shown in Table 3, $(\text{AOA } amoA + \text{AOB } amoA + \text{anammox} + nrfA)/\text{bacteria}$, $nrfA/(\text{narG} + \text{napA})$, and *nrfA* were the key factors for NH_4^+ -N transformation in phases I–V. The variable, $(\text{AOA } amoA + \text{AOB } amoA + \text{anammox} + nrfA)/\text{bacteria}$ showed a positive relationship with NH_4^+ -N transformation in phases I–II. The AOA *amoA* and AOB *amoA* genes are often regarded as NH_4^+ -N to NO_2^- -N oxidation markers, and *nrfA* is often regarded as a NO_3^- -N to NH_4^+ -N reduction makers.²⁴ Thus, results showed that the coupling of partial nitrification, anammox, and DNRA was involved in NH_4^+ -N conversion. The *nrfA/(\text{narG} + \text{napA})* group was the key functional group for NO_3^- -N consumption in phases III–V. Both *narG* and *napA* were regarded as marker genes for NO_3^- -N to NO_2^- -N in the first denitrification step. Hence, *nrfA/(\text{narG} + \text{napA})* and *nrfA* denoted NO_3^- -N reduction, showing a positive relationship and a negative relationship with NH_4^+ -N conversion, respectively. This result suggested that dissimilatory nitrate reduction to ammonium affected NH_4^+ -N conversion in phases III–V.

The NO_2^- -N transformation rates were jointly determined by *anammox/bacteria*, *nirK*, and $\text{AOB } amoA/(\text{nxrA} + \text{anammox} + \text{nirK} + \text{nirS})$ in phases I–V. The variable *anammox/bacteria* in the NO_2^- -N equation which was denoted NO_2^- -N consumption showed a positive relationship with NO_2^- -N transformation in phases I–II. The results suggested that *anammox* were the primary NO_2^- -N removal pathway under low TOC/TN ratios (≤ 0.10). The variable *nirK* genes were regarded as marker genes for NO_2^- -N to NO in the denitrification step, showing a positive correlation with NO_2^- -N conversion. The variable AOB *amoA/*

Table 3 Quantitative response relationships between nitrogen transformation rates ($\text{mg L}^{-1} \text{d}^{-1}$) and functional genes abundance (copies per g sludge) in long-term experiments. Anammox represent the absolute abundance of anammox bacterial 16S rRNA. Bacteria represent the absolute abundance of total bacterial 16S rRNA

Stepwise regression equations	R^2	p value
(TOC/TN = 0 and TOC/TN = 0.10)		
$\text{NH}_4^+-\text{N} = 385.638(\text{AOA } amoA + \text{AOB } amoA + \text{anammox} + \text{nr}fA)/\text{bacteria} + 313.386$	1.000	0.013
$\text{NO}_2^--\text{N} = 73.546\text{anammox}/\text{bacteria} + 458.162$	0.995	0.024
$\text{NO}_3^--\text{N} = -8679.981\text{nosZ}/\text{nirS} + \text{nirK} + 761.040$	0.983	0.008
(TOC/TN = 0.20, TOC/TN = 0.40, TOC/TN = 0.80)		
$\text{NH}_4^+-\text{N} = -2.709\text{nr}fA/(\text{narG} + \text{napA}) - 0.002\text{nr}fA + 1143.337$	0.997	0.008
$\text{NO}_2^--\text{N} = 8.067 \times 10^{-6}\text{nirK} - 246.61\text{AOB } amoA/(\text{n}xrA + \text{anammox} + \text{nirK} + \text{nirS}) + 475.431$	1.000	0.017
$\text{NO}_3^--\text{N} = 0.103(\text{nirK} + \text{nirS})/\text{AOB } amoA - 0.002\text{nr}fA + 1578.045$	0.982	0.005

($\text{n}xrA + \text{anammox} + \text{nirK} + \text{nirS}$) group which was denoted NO_2^--N accumulation showed a negative relationship with NO_2^--N conversion. This result indicated that the denitrification step was the primary factor which accounted for the NO_2^--N transformation at high TOC/TN ratios (≥ 0.20), while nitrification was inhibited in phases III–V.

The NO_3^--N transformation rates were collectively determined by $\text{nosZ}/(\text{nirS} + \text{nirK})$, $(\text{nirK} + \text{nirS})/\text{AOB } amoA$, and $\text{nr}fA$ in phases I–V. nirS and nirK genes are often regarded as NO_2^--N to NO genes. The $\text{nosZ}/(\text{nirS} + \text{nirK})$ in phases I–II was negatively associated with NO_3^--N transformation rates, suggesting that denitrification was not significant under low TOC/TN ratios (≤ 0.10). The $(\text{nirK} + \text{nirS})/\text{AOB } amoA$ in phases III–V was denoted NO_2^--N consumption showed a positive relationship with NO_3^--N conversion. The more NO_2^--N that was consumed, the more NO_3^--N was transformed; this was because lower NO_2^--N concentrations can reduce its toxic effects on denitrifiers.³²

Based on these results, the simultaneous presence of anammox, denitrification, and organotrophic anammox (DNRA) were confirmed in the anammox–SBR system under different TOC/TN constrains. This coupling of anammox, denitrification and DNRA can assist in the simultaneous removal of nitrogen and organic carbon in a single system, rather than over a sequential chain of treatments.⁴⁰

3.5. Molecular mechanism of nitrogen transformation pathways

Path analysis was further performed to explore the contribution of functional gene groups to the process of nitrogen removal in phases I–V. Path analysis revealed that $(\text{AOA } amoA + \text{AOB } amoA + \text{anammox} + \text{nr}fA)/\text{bacteria}$ has a direct positive effect on the NH_4^+-N transformation rate (0.216) under TOC/TN ratios ≤ 0.10 (Fig. 4 a). However, $\text{nr}fA/(\text{narG} + \text{napA})$ and $\text{nr}fA$ also has a lower direct negative effect on the NH_4^+-N transformation rate (-1.101 and -0.143 , respectively) under TOC/TN ≥ 0.20 . The indirect positive effect of $(\text{AOA } amoA + \text{AOB } amoA + \text{anammox} + \text{nr}fA)/\text{bacteria}$ via $\text{nr}fA$ on the NH_4^+-N transformation rate was 0.107. The indirect positive effect of $\text{nr}fA$ via $(\text{AOA } amoA + \text{AOB } amoA + \text{anammox} + \text{nr}fA)/\text{bacteria}$ on the NH_4^+-N transformation rate was 0.058, which was lower than the aforementioned indirect effect. These results suggested that $(\text{AOA } amoA + \text{AOB } amoA + \text{anammox} + \text{nr}fA)/$

bacteria was the better predictive variable and a key functional group for the NH_4^+-N transformation rate. The results also indicated that coupling nitrification and anammox was the primary factor behind NH_4^+-N removal under TOC/TN ratios ≤ 0.10 , while DNRA was the pathway contributing to NH_4^+-N accumulation under TOC/TN ≥ 0.20 .

The direct effect of $\text{anammox}/\text{bacteria}$ and nirK on NO_2^--N transformation rates were positive and values were 0.590 and 0.841, respectively. The direct effect of $\text{AOB } amoA/(\text{n}xrA + \text{anammox} + \text{nirK} + \text{nirS})$ on the NO_2^--N transformation rate was negative (-0.869) and was lower in strength than the positive direct effects. The indirect effect of $\text{anammox}/\text{bacteria}$ via $\text{AOB } amoA/(\text{n}xrA + \text{anammox} + \text{nirK} + \text{nirS})$ on the NO_2^--N transformation rate was positive (0.172), and the indirect effect of nirK via $\text{AOB } amoA/(\text{n}xrA + \text{anammox} + \text{nirK} + \text{nirS})$ on the NO_2^--N transformation rate was also positive (0.108) (Fig. 4b). However, the indirect effect of $\text{AOB } amoA/(\text{n}xrA + \text{anammox} + \text{nirK} + \text{nirS})$ via $\text{anammox}/\text{bacteria}$ and nirK on the NO_2^--N transformation rates were negative. The results showed that $\text{anammox}/\text{bacteria}$ was the key factor for NO_2^--N removal under TOC/TN ratios ≤ 0.10 , and nirK was the better predictive variable for NO_2^--N removal under TOC/TN ratios ≥ 0.20 . The results also indicated that anammox was the primary process responsible for NO_2^--N removal in phases I–II, while denitrification was the primary pathway responsible for NO_2^--N conversion in phases III–V, which was congruent with the discussion in Section 3.4.

It was found that $\text{nosZ}/(\text{nirS} + \text{nirK})$ and $\text{nr}fA$ had direct negative effects on the NO_3^--N transformation rates (-0.758 and -1.012 , respectively) in phases I–V. However, $(\text{nirK} + \text{nirS})/\text{AOB } amoA$ had positive effects on the NO_3^--N transformation rate (0.149) (Fig. 4c). The indirect positive effects of $(\text{nirK} + \text{nirS})/\text{AOB } amoA$ and $\text{nr}fA$ via $\text{nosZ}/(\text{nirK} + \text{nirS})$ were 0.032 and 0.133, respectively. The indirect negative effects of $(\text{nirK} + \text{nirS})/\text{AOB } amoA$ and $\text{nosZ}/(\text{nirK} + \text{nirS})$ via $\text{nr}fA$ were -0.234 and -0.117 , respectively. The results indicated that $(\text{nirK} + \text{nirS})/\text{AOB } amoA$ and $\text{nr}fA$ were the best predictive variable and a major contributing factor to the determination of the NO_3^--N transformation rate. The results also suggested that denitrification was not primary factors in phases I–V, while $\text{nr}fA$ and denitrification was the primary process responsible for NO_3^--N and NO_2^--N removal under at TOC/TN ratios ≥ 0.20 , supporting the results presented in Section 3.4 and in Table 3.

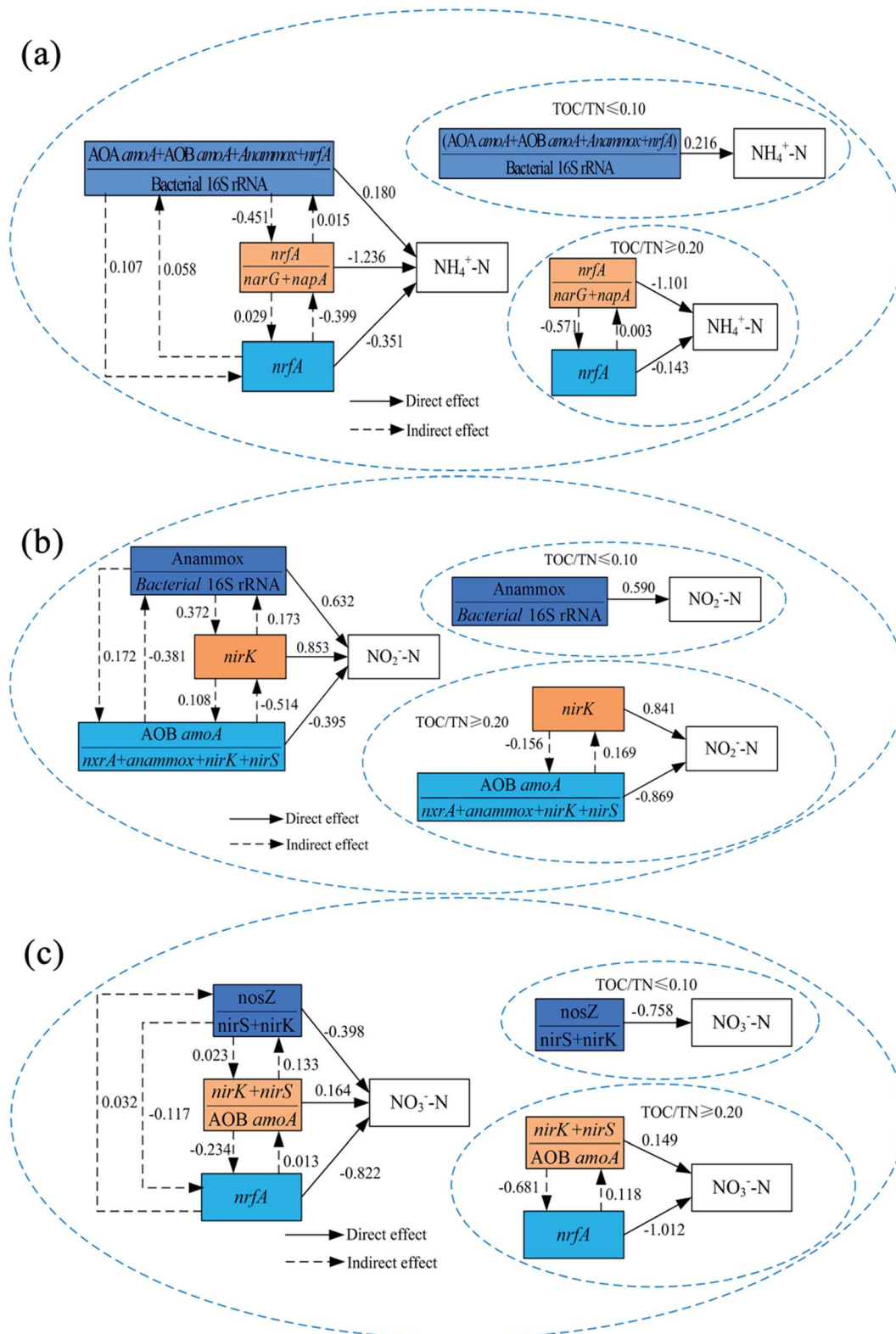


Fig. 4 Path diagrams estimating the effects of the functional gene groups on (a) NH_4^+ -N transformation rate, (b) NO_2^- -N transformation rate, and (c) NO_3^- -N transformation rate under different TOC/TN ratios constrains.

Compared with functional gene copy numbers, the results have evidenced that key functional gene groups can serve as integrative variables to characterize nitrogen transformation

rates in the organotrophic anammox process.⁴¹ On the quantitative molecular level, these analyses clearly revealed that the co-existence of autotrophic anammox, denitrification, and

DNRA (organotrophic anammox) could be useful for simultaneous nitrogen and TOC removal within the organotrophic niche.

3.6. Dynamics of bacterial communities and functional generalists

In this study, MiSeq sequencing was applied to investigate the dynamics of microbial communities and functional generalists in the organotrophic anammox process. After the filtration of raw sequences, 14 505–21 586 effective reads were obtained

from five samples. As shown in Table S2,[†] OTUs were in the range of 1112–1750, and increased in phases II–V as the TOC/TN ratio increased. Two estimators, which were Good's coverage and Simpson, showed unremarkable variation. However, Shannon, Chao 1, and ACE estimators varied significantly. These results indicated that TOC/TN stresses did not significantly effect the richness of the bacteria in the system, while they could significantly promote the diversity of related bacteria in the organotrophic anammox process. The

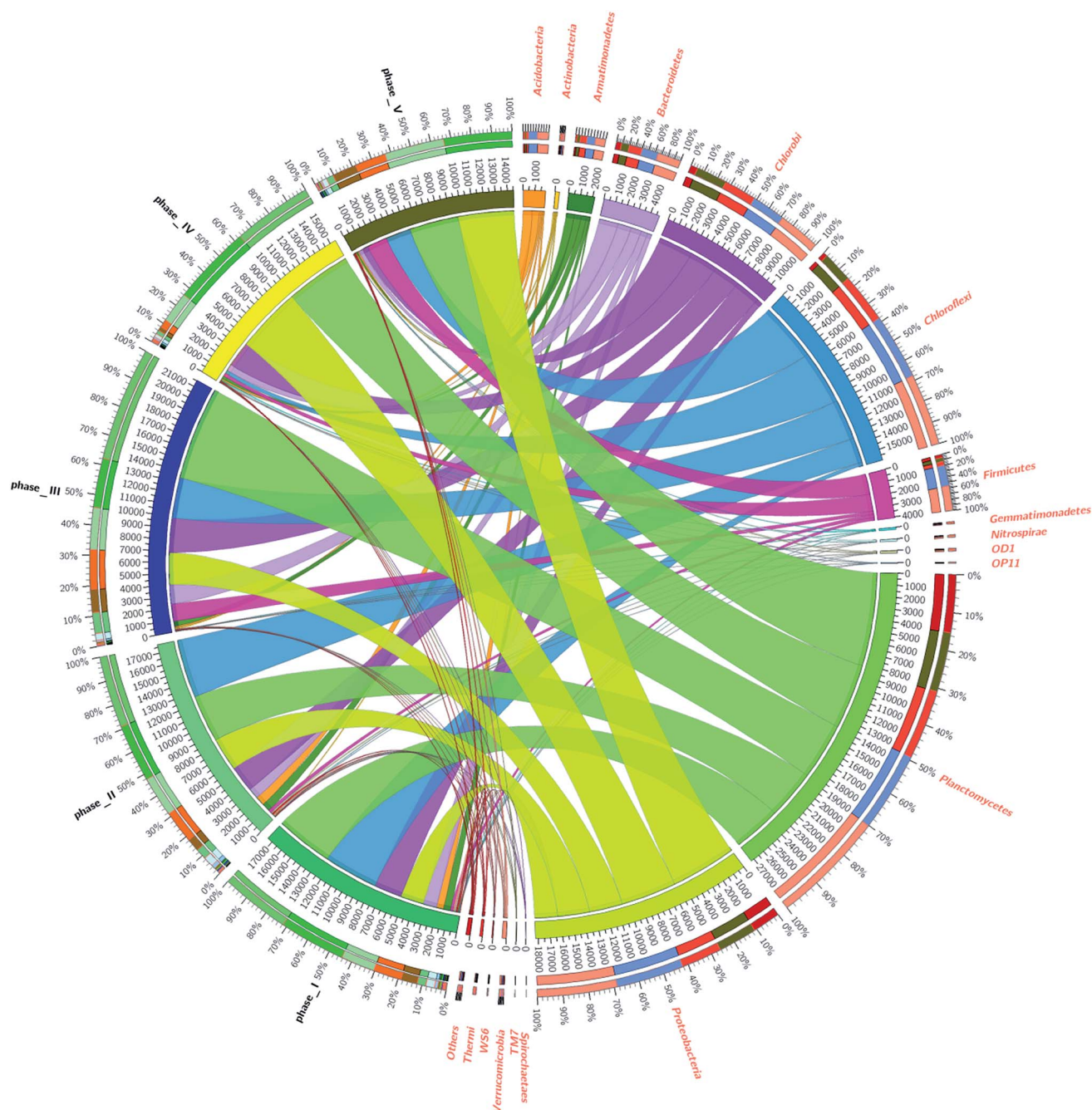


Fig. 5 Distribution of phyla in the different phase based on the taxonomy annotation from SILVA SSU database using RDP classifier. The thickness of each ribbon represents the abundance of each taxon. The absolute tick above the inner segment and relative tick above the outer segment stand for the reads abundances and relative abundance of each taxon, respectively. Others refer to those unclassified reads. The data were visualized using Circos (Version 0.67, <http://circos.ca/>).

rarefaction curves of five samples were also drawn in Fig. S1.† Results showed that the rarefaction curves did not reach a plateau in all phases, indicating that rare species could continue to emerge when the sequence depth exceed 14 000. As displayed in Fig. S2,† five samples belonged to four groups, indicating that lower TOC/TN ratios (<0.2) did not significantly influence microbial diversity.

In this study, effective sequences were assigned to phyla, class, order, family, and genera using RDP classifier *via* Silva SSU database. As shown in Fig. 5, a total of 15 bacterial phyla were identified. *Planctomycetes* was the most dominant phylum in all phases, accounting for 23.40–37.83% (averaging 31.25%). The other dominant phyla were *Proteobacteria* (11.45–36.92%, averaging 22.22%), *Chloroflexi* (1.95–28.91%, averaging 17.93%), and *Chlorobi* (3.54–14.01%, averaging 11.78%). Previous studies have reported that *Proteobacteria*, *Chloroflexi* and *Planctomycetes* were the significant phyla in the nitrification–anammox system.⁴² Fig. 5 clearly showed that *Planctomycetes* was more abundant than *Proteobacteria*, *Chloroflexi*, and *Chlorobi*, suggesting that *Planctomycetes* played the dominant role for nitrogen removal. In addition, as TOC/TN ratios increased from 0 to 0.20, the percentage of *Planctomycetes* increased from 28.48% to 37.83%. Then, it decreased to 29.59% as the TOC/TN ratio increased to 1.5%. The results indicated that *Planctomycetes* had higher tolerance for TOC/TN stresses, and that the appropriate addition of acetate and propionate was more favorable to enriching organotrophic anammox bacteria species in the phyla of *Planctomycetes*; these findings were consistent with the results reported in Section 3.1.

Notably, among *Proteobacteria*, β -*Proteobacteria* was the most dominant in all phases, followed by α -*Proteobacteria*, γ -*Proteobacteria*, δ -*Proteobacteria*, and ε -*Proteobacteria* (Fig. S3a†). Beside the class, the results from Fig. S3b and c† showed that the following major orders, namely *Ignavibacteriales*, *Clostridiales*, *Phycisphaerales*, *Brocadiales*, *Rhodobacterales*, and *Rhodocyclales*, and their corresponding families were shared by five phases, suggesting that these dominant populations played pivotal roles for nitrogen removal in the system.

As shown in Fig. S3d,† a total of 144 genera were assigned and 27 of them were dominant genera. Meanwhile, these genera were identified as belonging to 8 functional groups (Fig. 6). Among them, the anammox group involved “*Ca. Brocadia sinica*”, “*Ca. Jettenia asiatica*”, and “*Ca. Kuenenia stuttgartiensis*”. The relative abundance of “*Ca. Brocadia sinica*” were 4.32%, 4.43%, 4.73%, 5.3%, and 3.44%, respectively. Compared with “*Ca. Brocadia sinica*”, the relative abundance of “*Ca. Jettenia asiatica*” and “*Ca. Kuenenia stuttgartiensis*” were not detected in the phase I. These results indicated that “*Ca. Brocadia sinica*” was the dominant anammox bacteria species in the autotrophic system. With the addition of volatile fatty acids, the quantity of “*Ca. Brocadia sinica*” decreased. This was due to the ability of “*Ca. Brocadia sinica*” to oxidize volatile fatty acids.³⁴ During phases II–III, the percentage of “*Ca. Jettenia asiatica*” increased from 4.02% to 4.12%, while it decreased significantly in phase V. “*Ca. Kuenenia stuttgartiensis*” was detected at the lower TOC/TN ratio and decreased remarkably in phases IV and V. However, the quantity of “*Ca. Kuenenia stuttgartiensis*” increased from 3.01% to 3.67% with the further increased in the

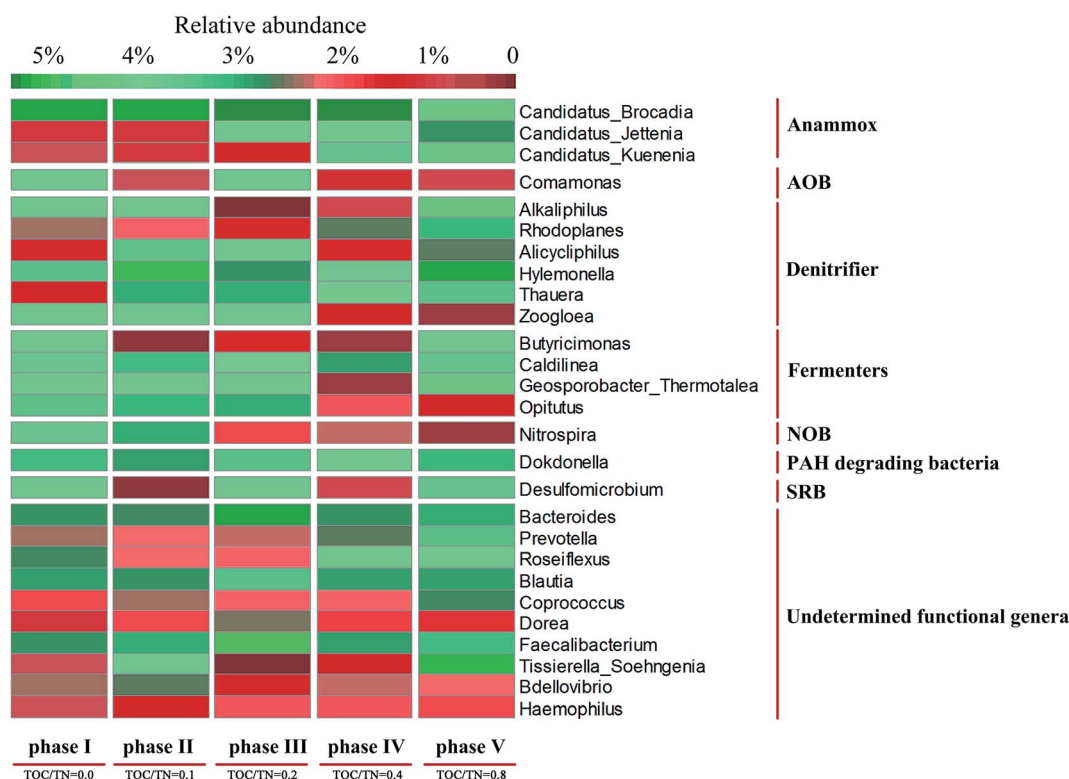


Fig. 6 The relative abundance of total 9 functional genera in five samples.

TOC/TN ratio from 0.4 to 0.8. This was due to the K-strategy survival ability of “*Ca. Kuenenia stuttgartiensis*”,⁴³ which prefers this strategy to low TOC conditions. However, “*Ca. Kuenenia stuttgartiensis*” was able to adapt to a higher TOC niche during the long-term acclimation. The appearance of “*Ca. Jettenia asiatica*” and “*Ca. Kuenenia stuttgartiensis*” in phases II–V resulted in a lack of significant variation in the anammox copy numbers despite suppression of the nitrogen removal activity in phase V.

Based on the results from the nitrogen treatment performance and MiSeq sequencing, it can be concluded that organotrophic anammox bacteria species have the capacity to oxidize acetate and propionate. In addition, “*Ca. Brocadia sinica*”, “*Ca. Jettenia asiatica*”, and “*Ca. Kuenenia stuttgartiensis*” have an organotrophic nature under the appropriate TOC/TN stress conditions. Furthermore, it was evident that higher TOC/TN ratios (>0.40) could result in the community succession of anammox species and alter the character of the microbial communities observed in this study.

4. Conclusion

Short- and long-term experiments revealed that the appropriate TOC/TN ratios enabled the maximum growth rate of the anammox to increase to 0.1356 d^{−1}. TOC biomass balance revealed that organotrophic anammox accounted for 14.76% of the nitrogen loss at a TOC/TN ratio of 0.20. Quantitative molecular analyses and pathway results confirmed that the coupling of anammox, DNRA, and denitrification was pivotal to the nitrogen transformation pathway in the organotrophic anammox process. MiSeq sequencing indicated that *Planctomycetes*, *Proteobacteria*, *Chloroflexi*, and *Chlorobi* were the most abundant phyla in the system. Furthermore, “*Ca. Brocadia sinica*” had tolerance to higher TOC stress conditions, and single environmental factors such as TOC/TN ratios could lead to microbial succession between “*Ca. Brocadia sinica*”, “*Ca. Jettenia asiatica*”, and “*Ca. Kuenenia stuttgartiensis*”. However, the quantitative molecular mechanism of the organotrophic anammox process in the anammox–SBR system needs further study using ¹³C-labeled DNA/RNA-SIP techniques. Moreover, the molecular mechanism for microbial succession between “*Ca. Kuenenia stuttgartiensis*”, “*Ca. Jettenia asiatica*”, and “*Ca. Kuenenia stuttgartiensis*” should also be further explored using metagenomic and metatranscriptomic approaches.

Acknowledgements

This study was financially supported by the National Natural Science Foundation of China (51308453) and the Science & Technology Innovation Program of Shaanxi Province (2011KTZB03-03-01).

References

- 1 A. A. Van de Graaf, P. de Bruijn, L. A. Robertson, M. S. Jetten and J. G. Kuenen, *Microbiology*, 1996, **142**, 2187–2196.
- 2 M. Strous, J. G. Kuenen and M. S. Jetten, *Appl. Environ. Microbiol.*, 1999, **65**, 3248–3250.
- 3 J. Guo, Y. Peng, L. Fan, L. Zhang, B. J. Ni, B. Kartal, X. Feng, M. S. Jetten and Z. Yuan, *Environ. Microbiol.*, 2015, **16**, 1–15.
- 4 T. Lotti, R. Kleerebezem, C. van Erp Taalman Kip, T. L. Hendrickx, J. Kruit, M. Hoekstra and M. C. van Loosdrecht, *Environ. Sci. Technol.*, 2014, **48**, 7874–7880.
- 5 B. Kartal, N. M. Almeida, W. J. Maalcke, H. J. Camp, M. S. Jetten and J. T. Keltjens, *FEMS Microbiol. Rev.*, 2013, 1–34.
- 6 S. Jenni, S. E. Vlaeminck, E. Morgenroth and K. M. Udert, *Water Res.*, 2014, **49**, 316–326.
- 7 C. Chen, X. Huang, C. Lei, T. C. Zhang and W. Wu, *Bioresour. Technol.*, 2013, **148**, 172–179.
- 8 S.-Q. Ni, J.-Y. Ni, D.-L. Hu and S. Sung, *Bioresour. Technol.*, 2012, **110**, 701–705.
- 9 C.-j. Tang, P. Zheng, C.-h. Wang and Q. Mahmood, *Bioresour. Technol.*, 2010, **101**, 1762–1768.
- 10 M. K. H. Winkler, J. Yang, R. Kleerebezem, E. Plaza, J. Trela, B. Hultman and M. C. M. van Loosdrecht, *Bioresour. Technol.*, 2012, **114**, 217–223.
- 11 B. Kartal, J. Rattray, L. A. van Niftrik, J. van de Vossenberg, M. C. Schmid, R. I. Webb, S. Schouten, J. A. Fuerst, J. S. Damsté and M. S. Jetten, *Syst. Appl. Microbiol.*, 2007, **30**, 39–49.
- 12 J. G. Kuenen, *Nat. Rev. Microbiol.*, 2008, **6**, 320–326.
- 13 B. Kartal, L. van Niftrik, J. T. Keltjens, H. J. Op den Camp and M. S. Jetten, *Adv. Microb. Physiol.*, 2012, **60**, 212.
- 14 X.-L. Huang, D.-W. Gao, Y. Tao and X.-L. Wang, *Chem. Eng. J.*, 2014, **253**, 402–407.
- 15 B. Kartal, L. Van Niftrik, J. Rattray, J. L. Van De Vossenberg, M. C. Schmid, J. S. Damsté, M. S. Jetten and M. Strous, *FEMS Microbiol. Ecol.*, 2008, **63**, 46–55.
- 16 H. Kamyab, M. F. M. Din, S. K. Ghoshal, C. T. Lee, A. Keyvanfar, A. A. Bavafa, S. Rezaia and J. S. Lim, *Waste Biomass Valorization*, 2016, 1–10.
- 17 H. Kamyab, M. F. M. Din, S. E. Hosseini, S. K. Ghoshal, V. Ashokkumar, A. Keyvanfar, A. Shafaghat, C. T. Lee, A. Asghar Bavafa and M. Z. A. Majid, *Clean Technol. Environ. Policy*, 2016, 1–11.
- 18 H. Kamyab, M. F. M. Din, A. Keyvanfar, M. Z. A. Majid, A. Talaiekhozani, A. Shafaghat, C. T. Lee, L. J. Shiun and H. H. Ismail, *Energy Procedia*, 2015, **75**, 2400–2408.
- 19 T. Zhang, M.-F. Shao and L. Ye, *ISME J.*, 2011, **6**, 1137–1147.
- 20 E. Isanta, T. Bezerra, I. Fernández, M. E. Suárez-Ojeda, J. Pérez and J. Carrera, *Bioresour. Technol.*, 2015, **181**, 207–213.
- 21 D. Shu, Y. He, H. Yue, L. Zhu and Q. Wang, *Bioresour. Technol.*, 2015, **196**, 621–633.
- 22 T. Lotti, R. Kleerebezem, Z. Hu, B. Kartal, M. Jetten and M. van Loosdrecht, *Water Res.*, 2014, **66**, 111–121.
- 23 R. Du, Y. Peng, S. Cao, C. Wu, D. Weng, S. Wang and J. He, *Bioresour. Technol.*, 2014, **162**, 316–322.
- 24 W. Zhi, L. Yuan, G. Ji and C. He, *Environ. Sci. Technol.*, 2015, **49**, 4575–4583.
- 25 C.-J. Tang, P. Zheng, L.-Y. Chai and X.-B. Min, *Chem. Eng. J.*, 2013, **230**, 149–157.

- 26 D. Shu, Y. He, H. Yue and Q. Wang, *Chem. Eng. J.*, 2016, **290**, 21–30.
- 27 C. K. Lee, C. W. Herbold, S. W. Polson, K. E. Wommack, S. J. Williamson, I. R. McDonald and S. C. Cary, *PLoS One*, 2012, **7**, e44244.
- 28 P. D. Schloss, S. L. Westcott, T. Ryabin, J. R. Hall, M. Hartmann, E. B. Hollister, R. A. Lesniewski, B. B. Oakley, D. H. Parks and C. J. Robinson, *Appl. Environ. Microbiol.*, 2009, **75**, 7537–7541.
- 29 S. J. Blazewicz, R. L. Barnard, R. A. Daly and M. K. Firestone, *ISME J.*, 2013, **7**, 2061–2068.
- 30 E. W. Rice, L. Bridgewater and A. P. H. Association, *Standard methods for the examination of water and wastewater*, American Public Health Association, Washington, DC, 2012.
- 31 P. Reichert, *Aquasim 2.0-user manual, computer program for the identification and simulation of aquatic systems*, Swiss Federal Institute for Environmental Science and Technology (EAWAG), 1998, p. 219.
- 32 Y. Pang, Y. Zhang, X. Yan and G. Ji, *Environ. Sci. Technol.*, 2015, **49**, 13550–13557.
- 33 D. F. Alwin and R. M. Hauser, *Am. Sociol. Rev.*, 1975, 37–47.
- 34 B. Kartal, M. M. Kuypers, G. Lavik, J. Schalk, H. J. Op den Camp, M. S. Jetten and M. Strous, *Environ. Microbiol.*, 2007, **9**, 635–642.
- 35 C.-J. Tang, P. Zheng, T.-T. Chen, J.-Q. Zhang, Q. Mahmood, S. Ding, X.-G. Chen, J.-W. Chen and D.-T. Wu, *Water Res.*, 2011, **45**, 201–210.
- 36 Y. Ahn, I. Hwang and K. Min, *Water Sci. Technol.*, 2004, **49**, 145–153.
- 37 Y. Liang, D. Li, X. Zhang, H. Zeng, Y. Yang and J. Zhang, *Bioresour. Technol.*, 2015, **193**, 408–414.
- 38 Y.-H. Ahn, *Process Biochem.*, 2006, **41**, 1709–1721.
- 39 M. Mußmann, I. Brito, A. Pitcher, J. S. S. Damsté, R. Hatzepichler, A. Richter, J. L. Nielsen, P. H. Nielsen, A. Müller and H. Daims, *Proc. Natl. Acad. Sci. U. S. A.*, 2011, **108**, 16771–16776.
- 40 G. D. Song, S. M. Liu, H. Marchant, M. M. M. Kuypers and G. Lavik, *Biogeosciences*, 2013, **10**, 6851–6864.
- 41 G. Ji, C. He and Y. Tan, *Ecol. Eng.*, 2013, **55**, 35–42.
- 42 Z.-r. Chu, K. Wang, X.-k. Li, M.-t. Zhu, L. Yang and J. Zhang, *Chem. Eng. J.*, 2015, **262**, 41–48.
- 43 W. R. Van der Star, W. R. Abma, D. Blommers, J.-W. Mulder, T. Tokutomi, M. Strous, C. Picoreanu and M. Van Loosdrecht, *Water Res.*, 2007, **41**, 4149–4163.